GATING OF THE Ca^{2+} CHANNEL AND THE KINETICS OF ELEMENTARY CALCIUM RELEASE EVENTS

IRINA BĂRAN

Biophysics Department, "Carol Davila" University of Medicine and Pharmaceutics, 8, Eroilor Sanitari Blvd, 050474 Bucharest, Romania

Abstract. By using a three-module decomposition of the inositol 1,4,5-trisphosphate receptor we describe both steady-state and dynamic features of the channel activity. Good agreement with published experimental data is obtained by estimating the errors introduced by missed events during single channel recordings. Inactivation as well as incremental detection at the receptor level can be well reproduced by the model in both deterministic and stochastic approaches. By simulating calcium release at individual sub cellular sites we find that the kinetics of elementary calcium events can be consistently explained by assuming that receptors are disposed as clusters with outputs located on the membrane of thin tubules of the endoplasmic reticulum, rather than assuming a spherical or hemispherical symmetry around a point source as generally accepted.

Key words: calcium, inositol 1,4,5-trisphosphate, ionic channel, model.

INTRODUCTION

Release of Ca^{2+} ions from the endoplasmic reticulum (ER) is a highly complex process, essential to many cellular events [2, 4]. Inside cells, calcium is released via the opening of its ER channel, the inositol 1,4,5-trisphosphate (IP_3) receptor (IP_3R), whose activity is tightly regulated by cytosolic factors such as Ca^{2+}, IP_3, and free ATP. Various models have been constructed [5, 7, 10, 13] that are able to explain most general features of the release process and thus have proved to be valuable tools in the study of the detailed mechanisms of intracellular calcium signaling. However, the high number of factors involved in the dynamic regulation of this channel activity as well as the limited data, which do not rarely give rise to discrepancies, have introduced essential difficulties in finding a convergence line toward the understanding of the mechanisms of channel gating and regulation of calcium release.

Received February 2004;
in final form January 2005.

ROMANIAN J. BIOPHYS., Vol. 13, Nos. 1–4, P. 17–29, BUCHAREST, 2003

With the use of a model of the IP_3R based on autonomous module decomposition of channel gating, we show that both the steady state and the dynamic activity of the channel can be accurately described by assuming that three gating elements operate independently and determine the channel to activate, inhibit or inactivate on different time scales.

MODEL FOR IP_3R GATING

As we have shown in a previous work [1], the activity of the type-1 IP_3 receptor (IP_3R1) can be accurately described by a 64-state system at thermal equilibrium, consisting of three independent gating modules, namely the activation, inhibition and inactivation modules. It is assumed that four sites regulate the fast gating kinetics, while two other sites regulate the slow kinetics of the receptor. The activation and inhibitory modules are driven each by Ca^{2+} binding to its activating and, respectively, inhibitory cytosolic site (S_a and S_i). In addition, kinetics of calcium binding at either site are independent of each other, but dependent on binding to the receptor of a specific factor, f_a or f_i, respectively. From a structural point of view, each gating module represents a channel domain that includes two regulatory sites: S_a and S_{fa} for the activating gate, S_i and S_{fi} for the inhibitory gate. Fig. 1 presents the state diagram of the IP_3R1 gating modules and the reactions assumed to regulate the activity of the channel.

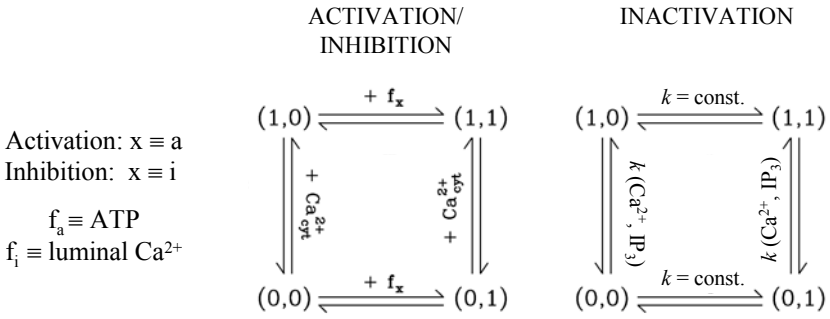

Fig. 1. – States and transitions within activation, inhibition and inactivation modules of the IP_3 receptor. Each state is described by the pair (O_{S1},O_{S2}) where O is the occupancy of the site S, i.e. 0, if the site has not bound the ligand, and 1 otherwise. In the inactivation module representation, k denotes reaction rate constant, which is either constant or depends on ligand concentration.

The fast kinetics of the channel are well represented [1] by an activation module driven by Ca^{2+} and ATP binding to their activating sites on the cytosolic region of the receptor, and by an inhibition module, regulated by Ca^{2+} binding to

one luminal and one cytosolic Ca^{2+} site of the receptor. One gate is associated to each module and a summary description of its regulation is given in Table 1.

Table 1

Gating modules of the IP_3 receptor and their regulation

Gating module	**Regulatory factors**	**States with open gate**
activating (fast)	cytosolic Ca^{2+} and ATP	(1,0) and (1,1)
inhibitory (fast)	cytosolic and luminal Ca^{2+}	(0,0)
inactivating (slow)	cytosolic Ca^{2+} and IP_3	(0,0) and (1,1)

STEADY STATE OPEN PROBABILITY OF THE IP_3R

In order to calculate the open probability of the channel at steady state, we have used first order kinetics for all binding- and dissociation-reactions, mass balance equations and thermodynamic equilibrium constraints, and assumed that two open states exist within the activation module, one open state within the inhibition module and two open states within the inactivation module (shown in Table 1). Full details of the calculation procedure are given in [1].

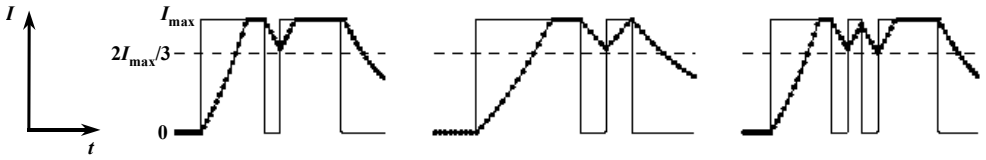

Fig. 2. – Typical events in single channel recordings as time evolution of the ionic current I through the channel. Channel activity is measured as events where the channel is open and conducts the current ($I > 0$) or is closed and blocks ions' passage ($I = 0$). The dotted line represents the recorded ionic current through the channel, the continuous line shows the actual channel activity (open/closed), and the dashed line indicates the current level $2I_{max}/3$.

We have to take into consideration that experimental data obtained with single channel recordings yield apparent, not real values, as a consequence of the technical inability to detect events with duration lower than a certain time limit. Generally the time resolution of this kind of determinations ranges between 40 and 500 μs. With the data [8, 9] used for our analysis the events with channel current variations smaller than one third of the current amplitude are not detected ($\Delta I < I_{max}/3$), which determines a detection limit $\tau_d \cong 0.3$ ms.

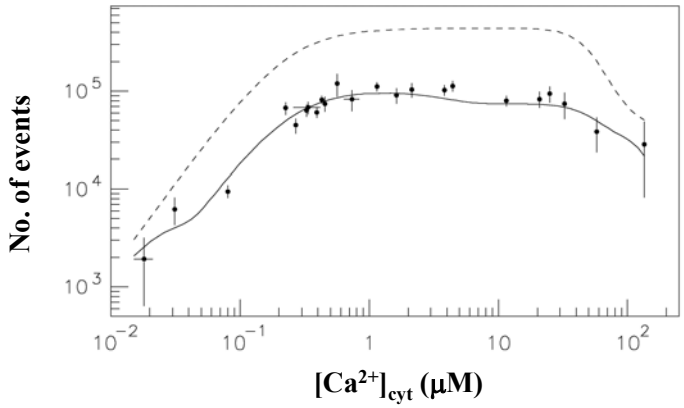

Fig. 3. – Actual and apparent number of open (or closed) channel events in a 1000 s – recording. Points and error bars are calculated based on open and close time data taken from [8], solid line is the theoretical fit based on the model and represents the apparent number of events, and dashed line shows the total number of events as calculated with our theoretical procedure.

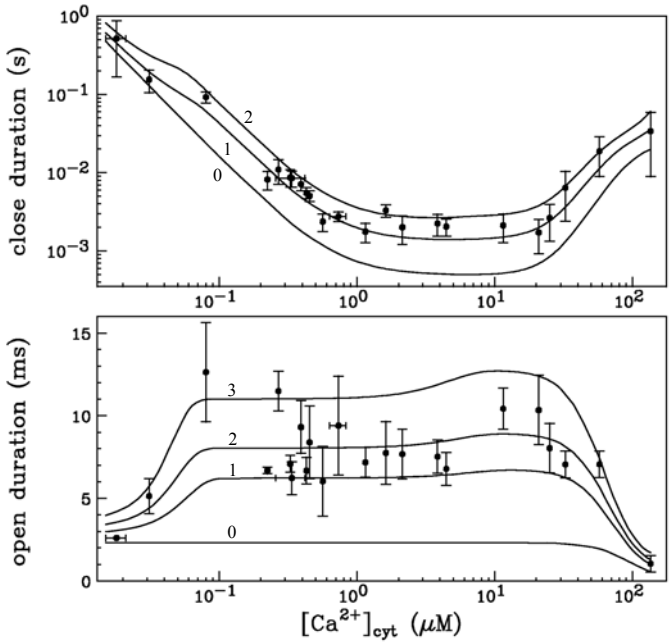

Fig. 4. – Ca^{2+}-dependence of the open- and closed- channel duration at 10 μM IP_3 and 500 μM ATP. Data are from [8]. In both panels the lowest line (numbered '0') corresponds to the actual value of the respective dwell time ($\tau_d = 0$), and curve '1' corresponds to a 0.2 ms resolution. In the upper panel, curve '2' is calculated with $\tau_d = 0.4$ ms. In the lower panel curves '2' and '3' are determined by $\tau_d = 0.3$ ms and $\tau_d = 0.4$ ms, respectively.

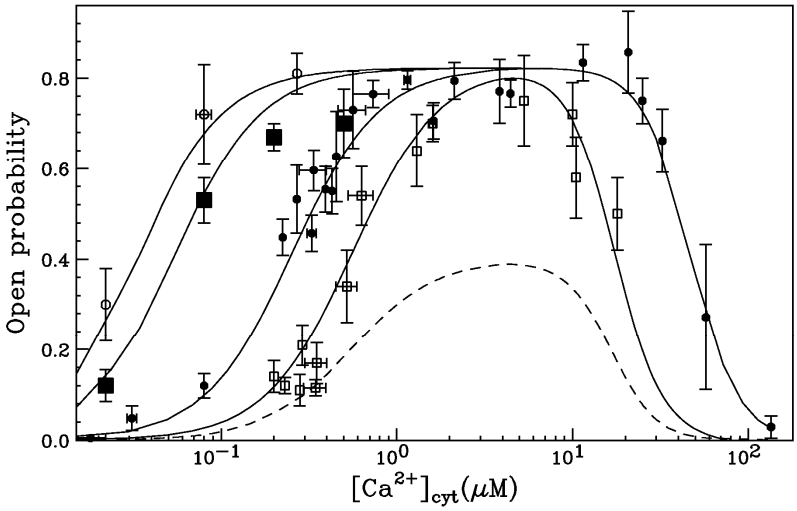

Fig. 5. – Apparent open channel probability at 10 μM IP_3, and 0–12 μM (small squares), 500 μM (filled circles), 4.8 mM (large squares), and 9.5 mM (open circles) ATP, and 0.2 μM Ca^{2+}_{ER} (solid lines) or 1 mM Ca^{2+}_{ER} (dashed line). Data are from [8, 9]. Curves are drawn according to the present analytical procedure by using $\tau_d = 0.3$ ms.

To calculate the errors introduced by missed events, we estimate the detection errors caused by successions of up to four undetectable events. Fig. 2 shows examples of one, two and three successive events with duration less than the experimental time resolution. An undetectable event is assumed to appear with the same probability all over the recording. By neglecting successions of more than 4 consecutive missed events one can determine the total number of events together with the number of missed events, and obtain by subtraction the apparent number of events during a certain time interval.

With this procedure one can calculate the apparent open and close dwell time, as well as the apparent open probability of the channel [1]. As shown in Figs. 3, 4 and 5, there is a very good agreement between our theoretical calculations and the experimental data. All parameter values used for the calculations are specified in [1].

CHANNEL INACTIVATION

It has been found that the IP_3 receptor undergoes an IP_3-and Ca^{2+}-dependent inactivation and that recovery from inactivation is slow, with a time constant of the order of tens of seconds [6, 11]. The underlying mechanisms are still not clear. Moreover, the existent models of the IP_3 receptor have avoided this issue and have

focused mainly on explaining steady state properties of the channel. The present model incorporates an inactivation gating component of the channel (see Fig. 1), which is able to reproduce the kinetics of the channel after repeated stimulation with pulses of IP_3.

In the simulations shown in Fig. 6 we have used a simplified scenario that mimics the variation of Ca^{2+} concentration at channel's mouth, as follows. We assume that during the first 40 ms of the stimulation IP_3 increases at a constant rate [5] so that to reach a 0.6 μM level at the end of this interval, then decays exponentially to the basal level, with a time constant of 1 s [5]. This kind of variation in the level of IP_3 follows closely the IP_3 pulse protocol in experiments with caged IP_3 [5, 11]. Ca^{2+} at channel's mouth is assumed to increase to 80 μM after channel opening [1] and, after a conducting period of 2.5 ms (close to the mean open time of the channel, see Fig. 4), decays exponentially to the basal level, with a time constant of 0.1 s [3, 12]. The basal levels of Ca^{2+} and IP_3 are considered as 50 nM and 20 nM, respectively. For the second pulse stimulation the same scenario is applied. Fig. 6 shows that with the model discussed above one obtains very good agreement with experimental findings on IP_3R inactivation [11].

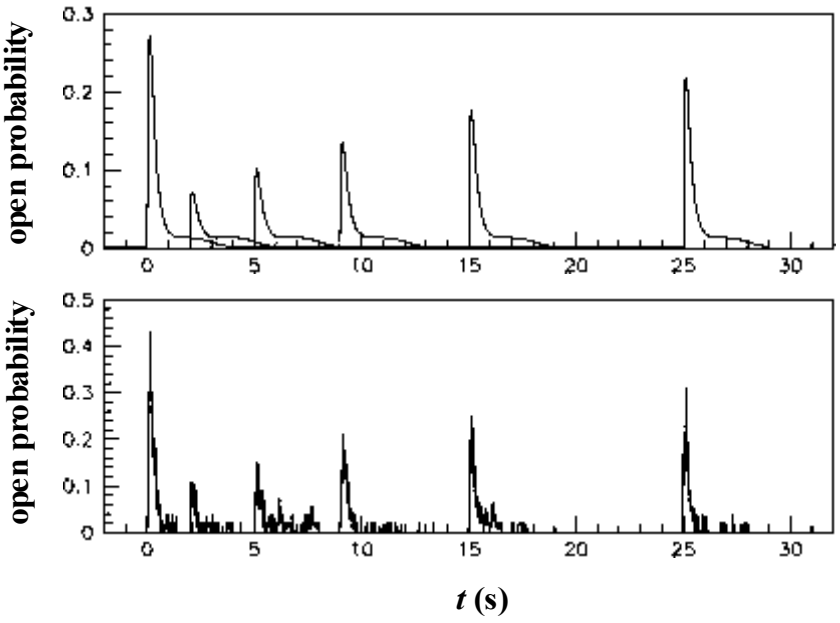

Fig. 6. – Deterministic solution (upper panel) and stochastic simulation (lower panel) according to a two-pulse 0.6 μM IP_3 stimulation protocol.

The model was tested also for the particular case of a small number of receptors since IP_3 receptors are organized as clusters of 10–30 channels [1, 13]. To describe this situation one has to approach the activity of a finite number of channels by stochastic simulations. A typical simulation of this kind is presented in Fig. 6, where the open probability is averaged on a group of 25 channels whose activities are simulated independently. For each state of a certain gating module a random sub unitary number is generated and compared to the transition probability according to the reactions shown in Fig. 1. At every instant, the open probabilities of the 25 channels are summated and the resulting quantity is divided by 25 to obtain the mean open probability of the cluster. The precise stochastic procedure is described in detail in [1].

It is evident that the highest degree (75%) of inactivation appears with the second IP_3 pulse applied 2 s after the first stimulation, which comes in agreement with the experimental results in [11]. Likewise, inactivation is less pronounced as the interval between pulses increases and the time scale is also in good agreement with the experimental one [11].

INCREMENTAL RESPONSES OF IP_3 RECEPTORS

It has been shown that incremental stepwise application of IP_3 or Ca^{2+} induces rapid adaptation of the IP_3 receptors and incremental responses that give rise to the so-called 'quantal' Ca^{2+} release. This definition of the phenomenon is based on the fact that low levels of stimuli (IP_3 or Ca^{2+}) cause only partial release, but further increasing of the stimulation level evokes more release.

Since the Ca^{2+}-induced Ca^{2+} release is a regenerative process due to the stimulatory effect of cytosolic Ca^{2+} on IP_3 receptor activity [2, 4, 7-9], quantal release appears as an unexpected paradox and recent experimental findings explain it by phasic or adaptive Ca^{2+} liberation from intracellular stores with similar sensitivities to IP_3 [3].

Our model agrees with this interpretation and can reproduce the characteristic of rapid adaptation at the receptor level. The simulations in Fig. 7 show how IP_3 receptors respond to incremental steps of Ca^{2+}, displaying a succession of open probability transients as would be expected in a quantal release process.

The behavior of groups of 50 or 250 channels follows in average the deterministic solution (obtained with a receptor number approaching infinity) but displays stochastic fluctuations that decrease with increasing the number of receptors. Thus the deterministic solution will correspond to the global cytosolic Ca^{2+} signal, while a 50-channel simulation will correspond to a local Ca^{2+} signal developed around an individual release site, a cluster of IP_3Rs.

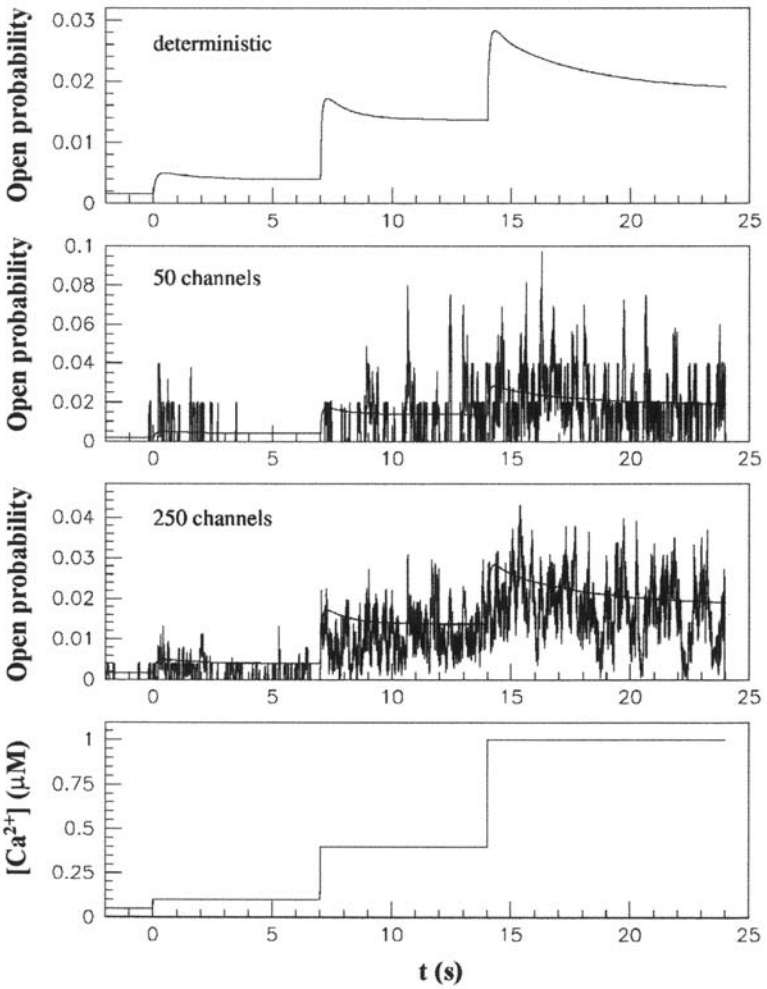

Fig. 7. – Deterministic solution and stochastic simulations of channel activity at constant IP_3 (0.6 μM) after stepwise increases of Ca^{2+}. The smooth line in the first three panels represents the deterministic solution of the system.

Ca^{2+} RELEASE AT INDIVIDUAL SITES

Theoretical approaches to release of calcium through ER channels have used various approximations whereby either the channel's mouth was considered as a point Ca^{2+} source placed in the center of the space or, in the case of clustered IP_3Rs, multiple sources were distributed on a planar ER region [13]. However, these models yield a 10-fold faster kinetics than found experimentally of the local calcium signals.

Our goal was to simulate release of calcium through a cluster of IP_3 placed on a thin tubule of the endoplasmic reticulum, so we have adopted a more appropriate geometry of Ca^{2+} release, as presented in Fig. 8, and used Scenario II (low K^+ gradient across the ER membrane) of the simulation method described in a previous work [1].

We consider a cluster of nine IP_3Rs placed on a thin (300–400 nm radius) tubule of the reticulum and calculate the time and space variation in the cytosolic calcium concentration following IP_3 stimulation. The center of the event is fixed by the highest increase in the local $[Ca^{2+}]$ detected on the scan line, and the concentration profile is calculated and averaged around that center over a distance of 400 nm along the scan line as in [12], yielding in this way a measure of the fluorescence signal.

In all simulations the actual scan line is a rather irregular volume comprising all the discrete elements having the center included in the parallelepiped of the 'regular' scan line. The length of the tubule segment, of 2–3 μm, is associated to the mean distance between neighbor release sites [3, 12]. The scan line is assumed to span the cytosol at an axial distance d_{line} = 150 nm under the tubule, and has the width r_{lat} = 133 nm and the depth r_{ax} = 300–400 nm [12]. The length of the scan line is determined by the limit of the simulated cytosolic depth (2–3 μm) where fixed boundary conditions ($[Ca^{2+}]$ = 50 nM) are applied (for details please see [1]). The center of the cluster is oriented under the angle α measured from the center of the scan line, and both centers are in the plane $y = 0$.

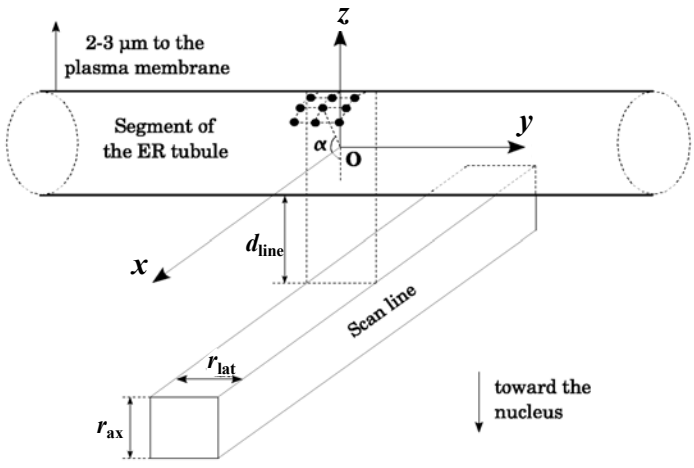

Fig. 8. – Geometry of calcium release. Clustered IP_3Rs are represented as small black circles on the surface of a reticulum cylindrical segment, and are 50 nm inter-spaced (both on the y axis and on the tubule circumference). The notations are explained in the text.

The simulation procedure described in [1] is strictly applied, except that the exogenous mobile calcium buffer is replaced with the calcium fluorescent indicator Calcium Green-1. Both endo- and exogenous mobile buffers have been included with total concentration 50 μM each, dissociation constant 10 and 0.26 μM, on-rate constant 10 and 1 $\mu M^{-1}s^{-1}$, and diffusion coefficient 15 and 18.4 $\mu m^2/s$, respectively. The endogenous fix buffer is present with total concentration 350 μM, dissociation constant of 10 μM and on-rate constant of 50 $\mu M^{-1}s^{-1}$. All concentrations are averaged every 5 ms.

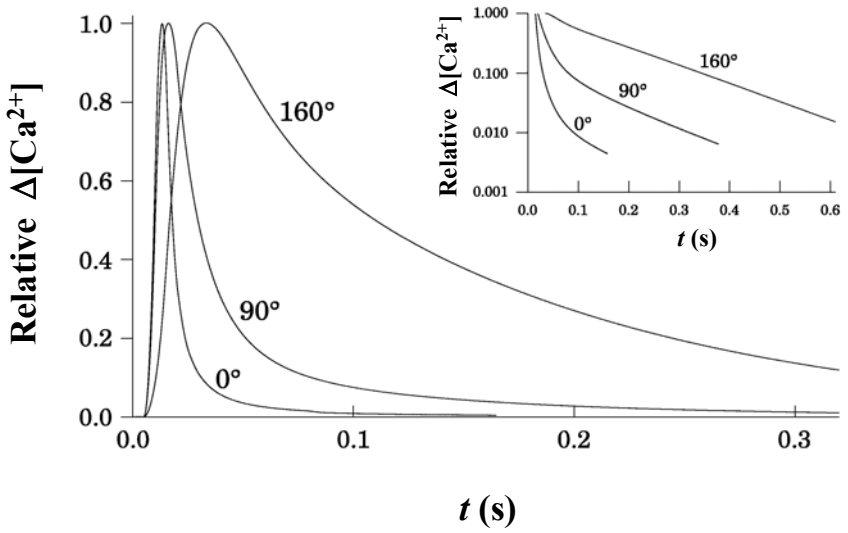

Fig. 9. – Simulated calcium signal with $\alpha = 0°$, 90° and 160°, respectively. Each trace is normalized to its maximum. All channels are assumed to open at $t = 0$ and remain open for the next 5 ms only. Tubule radius is 300 nm, and the cytosolic depth 2 μm. The inset shows calcium decay on logarithmic scale.

Experimentally, the half decay time in *Xenopus* oocytes was systematically found in the approximate range 0.06–0.14 s [3, 12]. The kinetics of the simulated calcium transients falls within the respective range only with 150–160° viewing, while with frontal imaging ($\alpha = 0$) the calcium transient is ten times faster. Fig. 9 shows the kinetics variation with the detection angle. Two exponential components of the decay phase are evident for each trace. The case $\alpha = 180°$ was not included because it yields a symmetric double event image, while we were interested mainly in the results of [12], where only images appearing as single site events have been selected.

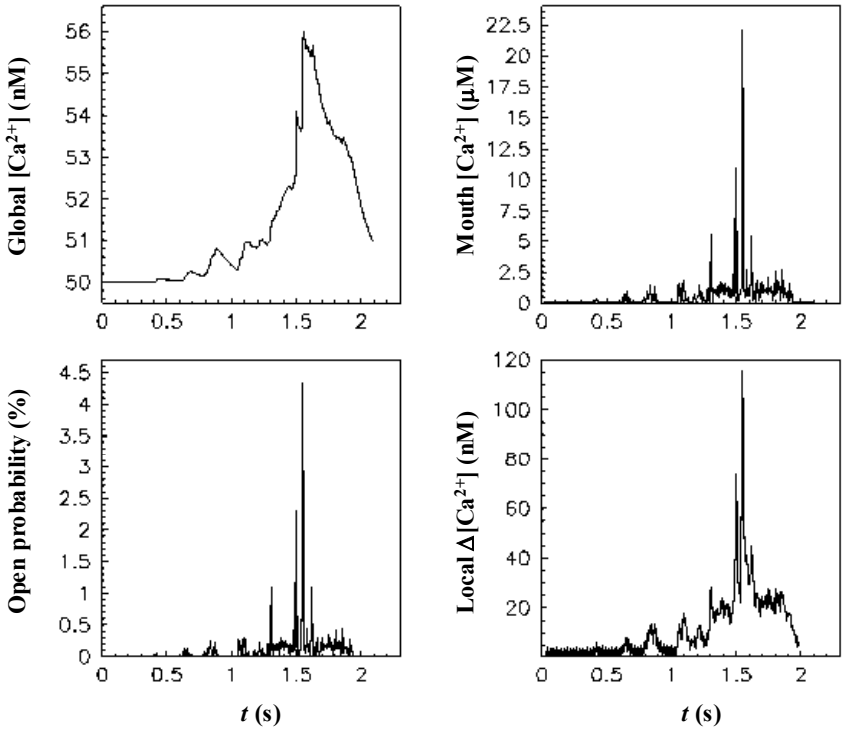

Fig. 10. – Simulation of calcium release, obtained by using the geometry presented in Fig. 8 and the full 64-state model of the IP_3R. Global Ca^{2+} signal is averaged over the cytosolic simulated volume, $[Ca^{2+}]$ at channel's mouth is the concentration in the volume element facing the central receptor in the cluster, open probability is averaged over all channels, and local $[Ca^{2+}]$ is obtained as in Fig. 9, with $\alpha = 90°$.

In the calculations presented above we were interested in the kinetics of local Ca^{2+} signals and did not use the IP_3R gating model. In the following simulation, shown in Fig. 10, we combine the same release geometry with the gating model and find that our model can reproduce the basic characteristics of both the local and global calcium transients. Increase of IP_3 from 20 nM (basal level) to 800 nM at t = 0.3 s induces calcium liberation after a latency period of 0.2 s. It has been shown experimentally that the latency following IP_3 stimulation ranges between 40 ms and several seconds. The latencies we obtained by repeated simulations were all included in this range. Short openings of a few channels in the cluster precede a prolonged period of release (≅ 0.9 s) ended by shut of all active channels. It is evident that high increases of Ca^{2+} at the open channel mouth (> 5 μM obtained by 10 ms-averaging) induce rapid channel inhibition and the open probability decreases within a few milliseconds to a low value. The average Ca^{2+} concentration over the simulated cytosolic volume extending 2 μm away from the ER tubule

displays a slower kinetics as compared to the local signal, due to the time required for diffusion into the cytosol of both the Ca^{2+} ions and the bound and not bound forms of the dye. Moreover, the global signal has a reduced amplitude and decays much more slowly, with a half-decay time of about 0.35 s. Macroscopic Ca^{2+} signals result from summation over numerous such Ca^{2+} transients emerging from sub cellular release sites. Therefore, the knowledge of the behavior of an individual site is of extreme physiological importance.

CONCLUSION

We show that a simple model of IP_3R gating operated by three independent modules can explain the Ca^{2+}, IP_3 and ATP dependence of the open probability, open and close dwell times of the channel at steady state, as well as channel inactivation and recovery from inactivation on a long time scale, or the quantal characteristic of calcium release.

Kinetic studies on Ca^{2+} release have proved that the Ca^{2+} channel is subjected to an IP_3- and Ca^{2+}-dependent slow inactivation, which are reproduced here with the contribution of a slow gating module showing constant open gate probability at steady state. This element, termed inactivation module, is, therefore, assumed to be driven by Ca^{2+}- and IP_3- dependent reactions, yet yielding in steady state a constant (*i.e.,* not dependent on Ca^{2+}, IP_3 and ATP concentrations) open probability of the inactivation gate. The reaction scheme of the inactivation module shown in Fig. 1 satisfies this condition. Moreover, it can explain how the channel recovers within tens of seconds from inactivation induced by a short pulse of IP_3, and can also explain the paradox of the quantal calcium release.

By simulating Ca^{2+} release at individual sites and considering that IP_3 receptors are disposed as clusters on the surface of thin tubules of the endoplasmic reticulum we obtain very good agreement with the experimental findings on the biphasic kinetics of the elementary calcium events. Thus, the discrepancy between theory and experiment with regard to the kinetics of elementary calcium events can be avoided if it is assumed that the Ca^{2+} source is located on the membrane of thin tubules, not on a planar portion of the reticulum or at the center of a spherically symmetric space.

As the minimum half-decay time of the Ca^{2+} transients was about 60 ms as obtained by scanning of a region located between 3 and 6 μm under the membrane, we conclude from our determinations that no release event is there detected frontally or laterally, meaning that receptors within this region are not operative, while the functional receptors are disposed at the boundary of the IP_3R-rich region, namely at a cytosolic depth of either ≅2 μm or ≅8 μm, and oriented to opposite directions. This type of spatial organization of the IP_3 receptors may have important implications in the physiology of intracellular signaling, as for example in inducing capacitive calcium influx or gene expression in the nucleus [2, 4].

REFERENCES

1. BARAN, IRINA, Integrated luminal and cytosolic aspects of the calcium release control, *Biophys. J*., 2003, **84**, 1470–1485.
2. BERRIDGE, M.J., Inositol trisphosphate and calcium signaling, *Nature*, 1993, **361**, 315–325.
3. CALLAMARAS, N., I. PARKER, Phasic characteristic of elementary Ca^{2+} release sites underlies quantal responses to IP_3, *EMBO J*., 2000, **19**, 3608–3617.
4. CLAPHAM, D.E., Calcium signaling, *Cell*, 1995, **80**, 259–268.
5. De YOUNG, G.W., J. KEIZER, A single-pool inositol 1,4,5-trisphosphate-receptor-based model for agonist-stimulated oscillations in Ca^{2+} concentration, *Proc. Natl. Acad. Sci. USA*, 1992, **89**, 9895–9899.
6. HAJNŐCZKY, G., A.P. THOMAS, The inositol trisphosphate calcium channel is inactivated by inositol trisphosphate, *Nature*, 1994, **370**, 474–477.
7. KAFTAN, E.J., BARBARA E. EHRLICH, J. WATRAS, Inositol 1,4,5-trisphosphate and calcium interact to increase the dynamic range of $InsP_3$ receptor-dependent calcium signaling, *J. Gen. Physiol*., 1997, **110**, 529–538.
8. MAK, D.-O.D., S. McBRIDE, J.K. FOSKETT, Inositol 1,4,5-tris-phosphate activation of inositol 1,4,5-trisphosphate receptor Ca^{2+} channel by ligand tuning of Ca^{2+} inhibition, 1998, *Proc. Natl. Acad. Sci. USA,* **95,** 15821–15825.
9. MAK, D.-O.D., S. McBRIDE, J.K. FOSKETT, ATP regulation of type 1 inositol 1,4,5-trisphosphate receptor channel gating by allosteric tuning of Ca^{2+} activation, J. Biol. Chem., 1999, **274,** 22231–22237.
10. MORARU, I.I., E.J. KAFTAN, BARBARA E. EHRLICH, J. WATRAS, Regulation of type 1 inositol 1,4,5-trisphosphate-gated calcium channels by $InsP_3$ and calcium, *J. Gen. Physiol*., 1999, **113**, 837–849.
11. PARKER, I., I. IVORRA, Inhibition by Ca^{2+} of inositol trisphosphate-mediated Ca^{2+} liberation: a possible mechanism for oscillatory release of Ca^{2+}, *Proc. Natl. Acad. Sci. USA*, 1990, **87**, 260–264.
12. SUN, X.-P., N. CALLAMARAS, J.S. MARCHANT, I. PARKER, A continuum of $InsP_3$ mediated elementary Ca^{2+} signalling events in *Xenopus* ocytes. *J. Physiol*., 1998, **509**, 67–80.
13. SWILLENS, S., GENEVIEVE DUPONT, L. COMBETTES, P. CHAMPEIL, From calcium blips to calcium puffs: theoretical analysis of the requirements for interchannel communication, *Proc. Natl. Acad. Sci. USA*, 1999, **96**, 13750–13755.